JOURNAL OF GEOPHYSICAL RESEARCH, VOL. 108, NO. C3, 3092, doi:10.1029/2001JC000982, 2003

Variational assimilation of SSH variability from TOPEX/POSEIDON and ERS1 into an eddy-permitting model of the North Atlantic

Armin Köhl[1] and Jürgen Willebrand
Institut für Meereskunde Kiel, Kiel, Germany

Received 16 May 2001; revised 17 September 2002; accepted 30 September 2002; published 20 March 2003.

[1] A first step for improving the climatological state of high-resolution general circulation models by means of data assimilation is presented. A method developed for the assimilation of statistical characteristics into chaotic ocean models is applied to assimilate SSH variability from TOPEX/POSEIDON and ERS1 in association with temperature and salinity from the World Ocean Atlas 1997 in order to estimate the underlying mean circulation. The method requires a parameterization of SSH variability which derives from the approach of Green and Stone. By estimating initial conditions for temperature and salinity, a mean state is achieved which, although not fully consistent with the altimetric and climatological data, is markedly improved on time scales of one year in comparison to the control run. The assimilation of SSH variability data introduces complementary information about the main frontal structures consistent with climatological observations. The state is however not an equilibrium state and returns back to the first guess quasi-equilibrium state for longer integration periods. *INDEX TERMS:* 4255 Oceanography: General: Numerical modeling; 4263 Oceanography: General: Ocean prediction; 4532 Oceanography: Physical: General circulation; 4520 Oceanography: Physical: Eddies and mesoscale processes; 4528 Oceanography: Physical: Fronts and jets; *KEYWORDS:* data assimilation, statistical moments, North Atlantic Ocean, primitive-equation model, eddy permitting

Citation: Köhl, A., and J. Willebrand, Variational assimilation of SSH variability from TOPEX/POSEIDON and ERS1 into an eddy-permitting model of the North Atlantic, *J. Geophys. Res.*, *108*(C3), 3092, doi:10.1029/2001JC000982, 2003.

1. Introduction

[2] Altimetric data have become an important source of information about the ocean circulation. In particular, the spatial and temporal coverage of the global ocean is superior to most other data sources. Although the measurements are restricted to the ocean surface, strong vertical coherence within the upper ocean allows one to infer information about the subsurface region. An optimal method for the extraction of information is given by the assimilation of data into a general circulation model. Two different approaches are available and widely used, namely the Kalman filter and the adjoint method. Both originate from the same principle, and both are limited by the imperfect knowledge of the error covariances. Most applications for the assimilation of SSH anomalies are based on simplifications of the extended Kalman filter and employ various extrapolation schemes to account for spatial coherence of the error covariance matrix [*Oschlies and Willebrand*, 1996; *Cooper and Haines*, 1996; *Evensen and van Leeuwen*, 1996; *Gavart and De Mey*, 1997]. An application of the method of *Oschlies and Willebrand* [1996] demonstrates that the variability is improved while the mean state is effectively kept invariant [*DYNAMO Group*, 1997]. The method needs the mean SSH which is calculated from a reference run. Since the Gulf Stream path is distinctly different in the model than the observed path, solely improving the variability results in an unphysical interplay of the mean and the transient parts of the flow. Additional independent information about the mean state is therefore necessary, and was included by *Killworth et al.* [2001] in this scheme with considerable success.

[3] It is not clear to what extent multiple stable equilibria of the Gulf Stream system or model deficiencies account for differences to the observed data [*Dijkstra and Molemaker*, 1999]. By minimizing a cost function the adjoint method searches for the trajectory of a given dynamical system that fits the observations optimally so that the consistency of the solution with the dynamical equations is guaranteed. This enables the construction of states that more closely represent the observations which, however, may not be equilibrium states.

[4] The application of the adjoint method with high-resolution ocean models is not straightforward since these models obey chaotic dynamics with limited predictability.

[1]Now at Scripps Institution of Oceanography, La Jolla, California, USA.

0148-0227/03/2001JC000982

The stability of their tangent linear models (this includes adjoint models) is characterized by positive Lyapunov exponents which also characterize the limit of predictability of the model [*Kazantsev et al.*, 1998; *Kazantsev*, 1999]. Exponential growth of the adjoint model can be related to an increasing number of secondary minima of the cost function [*Köhl and Willebrand*, 2002, hereafter KW] which prevents the convergence of the adjoint method. Applications for the assimilation of altimeter data in high-resolution models have therefore been restricted to very short time spans of a few months [*Schröter et al.*, 1993; *Morrow and De Mey*, 1995], which are too short to allow signals to propagate into the deep ocean. The method of KW allows the extension of the assimilation period by defining the adjoint method on the basis of statistical quantities. In this paper the method is applied to assimilate sea surface height (SSH) variability into an eddy permitting model of the North Atlantic ocean.

[5] Patterns and amplitudes of annual SSH variability are intimately related to the underlying quasi-stationary mean circulation as described by *Stammer* [1997]. The close link between the mean and the variable part therefore can in principle be utilized in reverse order for the estimation of the mean state from the variable part of the circulation by means of data assimilation. That link also serves as a starting point for recent eddy parameterizations [*Treguier et al.*, 1997]. In the following application of the KW approach, a parameterization based on *Green* [1970] and *Stone* [1972] is included in the derivation of the adjoint model for statistical quantities. The main emphasis of this study is to show the feasibility of assimilating altimetric SSH variability to improve modeled climatological mean states by parameter estimation and for state estimations with high resolution models.

[6] After a brief review of the methodology, the forward and the adjoint models are presented in section 3. The parameterization for the SSH variability is presented in section 4. The results of a 1 year assimilation are discussed with some emphasis on the effect of the parameterization in section 5 followed by a concluding discussion.

2. Method

[7] The adjoint method used in this study was designed to allow for the assimilation of statistical moments of data into chaotic ocean models. It is an extension of the original formulation of *Le Dimet and Talagrand* [1986]. The basis of the method is the assumption that the dynamics of ocean models are decomposable into different time scale regimes associated with different ranges of predictability. Averaged quantities are assumed to be more predictable. The adjoint model derives from a separate model that describes the mean state and that features long-term predictability. Only a short outline of the technique is given in the following. A high-resolution model with short-term predictability is employed to calculate optimal estimates of single realizations of statistical moments. A coarse resolution twin version of the eddy-resolving model is used to approximate an independent model for the statistical moments used in the variational method as a strong constraint. This model is introduced to describe a predictable part of the evolution. A detailed derivation is described by KW.

[8] The basic concept is to employ a high-resolution model with short-term predictability to calculate the evolution of the state vector x according to

$$\frac{dx}{dt} = f(x, \alpha, t), \tag{1}$$

depending on the parameter vector α. Estimates of single realizations of statistical moments that enter the cost function are calculated from the solution of this model. A separate model for the mean state is employed for the construction of the adjoint. Coarse resolution twin version

$$\frac{dX}{dt} = F(X, \alpha) \tag{2}$$

of the eddy-resolving model is used to approximate this model for the mean state. The adjoint derives from an expansion at moments $\bar{x}$ calculated from the high-resolution model. The scheme then reads:
minimize

$$J(\alpha) = \frac{1}{2}(\alpha - \alpha_b)^T B^{-1}(\alpha - \alpha_b) + \frac{1}{2}(H\bar{x} - y)^T O^{-1}(H\bar{x} - y) \tag{3}$$

respecting the forward model

$$\frac{dx}{dt} = f(x, \alpha, t) \tag{4}$$

and the adjoint to the coarse resolution version

$$-\frac{d\lambda}{dt} = \partial_X F^{\dagger}(\bar{x}, \bar{\alpha})\lambda + H^T O^{-1}(H\bar{x} - y), \tag{5}$$

where $\bar{x}$ is a time mean and spatial average to the coarse grid, O is the error covariance of statistical moments y of observations, B is the error covariance of the background information α_b of the parameter α and H is the observation operator. The adjoint uses only temporally and spatially averaged information originating from the high resolution forward model. The estimated gradient and parameter improvements calculated by the descent step are therefore time independent and on the coarse resolution grid.

3. Numerical Models

[9] The primitive-equation ocean circulation model is based on the 1/3° CME model configuration developed by *Bryan and Holland* [1989]. It makes use of the revised code described by *Pacanowski et al.* [1993]. The domain of high-resolution forward model and the coarse resolution twin covers the Atlantic Ocean basin from 15°S to 65°N. Both models have 30 levels and share the same vertical grid spacing which increases smoothly from 35 m at the surface to 250 m below 1000 m. Buffer zones of 5 points width are applied on the closed boundaries where salinity and temperature are restored to data taken from *Levitus* [1982]. The northern boundary condition is supplemented in the Denmark Strait by actual section data [*Döscher et al.*, 1994].

3.1. Forward Model

[10] The model configuration is essentially identical to that described by *Oschlies and Willebrand* [1996]. A review of experiments and results of the CME configuration is given by *Böning* [1996]. The model is forced with the monthly mean wind stresses of *Hellerman and Rosenstein* [1983] and the heat flux is formulated according to the linear approximation of *Han* [1984]. Surface fluxes of fresh water are specified by relaxation to the monthly mean salinity values of *Levitus* [1982]. The horizontal grid spacing is 1/3° in meridional and 2/5° in zonal direction. Horizontal mixing is parameterized by biharmonic friction. Constant coefficients for viscosity and diffusivity are chosen as 2.5×10^{19} cm^4/s. In the vertical, Laplacian mixing is used with constant coefficients of 0.3 cm^2/s for diffusion and 10 cm^2/s for viscosity. Convection is parameterized by increasing the vertical mixing coefficients to 10^4 cm^2/s at places in the water column where static instability is detected.

3.2. Adjoint Model

[11] The high-resolution and the coarse resolution twin model are based on basically the same source code. The horizontal grid spacing is 1° in meridional and 1.2° in zonal direction. Unlike in the forward model, horizontal mixing is parameterized by harmonic friction with coefficients chosen as 5×10^8 cm^2/s to prevent the tangent linear model from developing unstable modes. The adjoint model was constructed with aid of the automatic code compiler TAMC [*Giering and Kaminski*, 1998]. In order to prevent a computational mode in the adjoint which results from the Euler coupling steps in the forward model [*Sirkes and Tziperman*, 1997], the forward code is modified to perform only leapfrog steps. Divergence of the two decoupled modes is not observed, and the adjoint variables asymptotically approach a stationary solution. As described in KW, prognostic variables as well as air-sea thermohaline and momentum fluxes of the forward model were averaged to the coarse grid, and only their temporal mean values enter the adjoint. The topography was derived from the high-resolution representation with the same spatial averaging procedure completed by an additional removal of holes and the restoration of islands. The seasonal cycle is removed in the adjoint, which is the adjoint to a model for the mean circulation. Including a seasonal cycle into the adjoint formalism would require the formation of ensemble mean values in order to eliminate the transient eddy component from the seasonal signal. The standard formulation of mixing in case of static instabilities makes the mixing coefficients effectively time dependent. By analogy to the treatment of the forcing, convection is parameterized in the adjoint by temporally and spatially averaging the mixing coefficients of the forward model.

[12] For the descent algorithm the variable storage minimization algorithm M1QN3 by *Gilbert and Lemaréchal* [1989] was chosen as a good compromise in terms of storage requirements between conjugated gradient and quasi-Newton methods. Gradients calculated by the coarse resolution model are interpolated by bicubic spline to the grid of the 1/3° model before descent steps were performed.

[13] Integration periods of several years are desirable in order to define statistical moments, however, test runs show that the assimilation period is limited to a range of about 1 year. An exponential increase of the Lagrangian multipliers starts after about a year of backward integration. Exponential increasing Lagrangian multipliers indicate a limit of predictability and are related to positive eigenvalues of the adjoint operator. In the method of KW, weaker gradients and lower extreme values of the velocity fields, in combination with higher values for mixing coefficients of the adjoint, prevent in general the development of unstable modes for integration periods of several years. In the present model, spatial gradients and extreme values of the velocity fields are, even after averaging, still large enough to allow for the development of instabilities. In agreement with this assumption, no instabilities were found for periods of several years if averaged prognostic variables originate from a coarse resolution forward model run.

4. Parameterization for SSH Variability

[14] Our statistical approach of the adjoint method requires a closed set of equations for all statistical moments included in the cost function, which in our case includes the second-order moment SSH variability. Approximating the statistical model by a low-resolution model twin as in KW requires an additional physical relation for the inclusion of higher-order moments. A simple parameterization approach as described in KW is followed to mimic a model for the prediction of rms SSH variability. The idea is to search for a relation that expresses second-order moments in terms of mean values. This parameterization forms together with coarse resolution model the set of equations for the mean state and the SSH variability.

[15] For the inclusion of rms SSH variability, σ_{SSH}, as a second-order moment, the eddy variability is parameterized in terms of the density structure derived from the mean temperature and salinity distribution. The generation of eddies is closely related to the stability properties of the mean current. Eddy energies calculated from tracked drifting buoys [*Richardson*, 1983; *Krauss and Käse*, 1984] and altimeter data [*Stammer*, 1997] indicate the major frontal zones as the primary location for the occurrence of variability. Outside the tropical regime, spectral characteristics of altimetric data from TP analyzed by *Stammer* [1997] suggest baroclinic instability as the dominant source of variability in accordance with the spectral relations of geostrophic turbulence. *Treguier et al.* [1997] shows that the depth-integrated rms eddy velocity can be related to the Richardson number Ri in the main regions of variability. The approach used in this study was originally derived on basis of the theory of baroclinic instability by *Green* [1970] and *Stone* [1972] who described the eddy velocity in terms of horizontal and vertical density gradients of the mean flow. Employing the thermal wind balance for the calculation of the vertical velocity shear, the relation reads

$$\sigma_{SSH} = \frac{\gamma}{\Delta z} \int_{110m}^{1250m} \frac{1}{\sqrt{Ri}} dz = \frac{\gamma}{H} \int_{110m}^{1250m} \sqrt{\frac{g\left(\rho_y^2 + \rho_x^2\right)}{f_o^2 \rho_o \rho_z}} dz, \qquad (6)$$

where Δz is the depth interval, f_o is the Coriolis parameter of a central latitude, ρ is the density, ρ_o is a reference density, and the length γ is the coefficient of proportionality.

[16] The impact of employing this relation for the assimilation of rms SSH variability in regions where the model

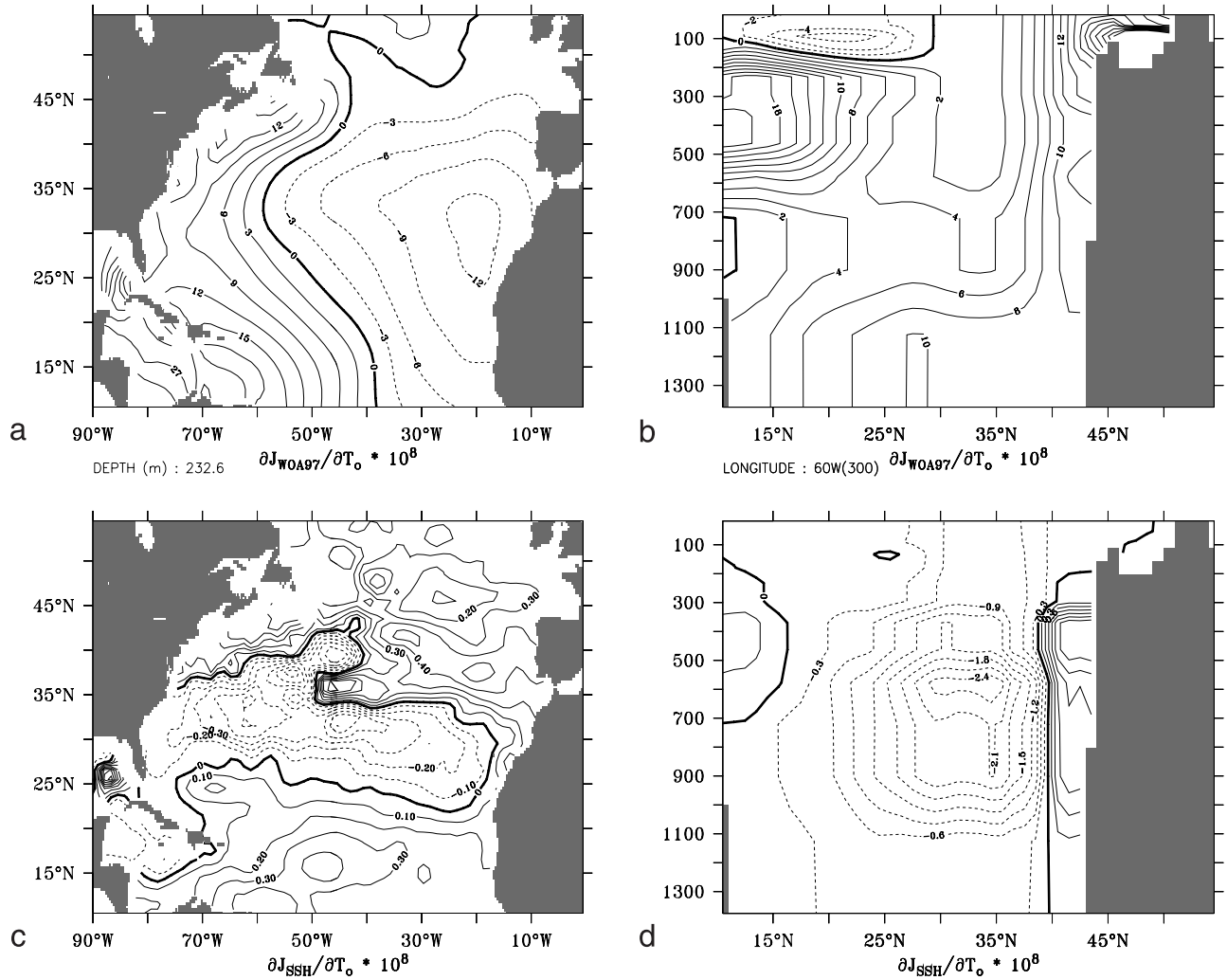

Figure 1. Cost function gradients with respect to the temperature initial condition. The part J_{WAO97} (a–b) measures the difference of annual mean temperature and salinity values to the WOA97 data (in 1/°C), and $J_{\sigma_{SSH}}$ (c–d) measures the difference of the rms SSH variability. The horizontal level in Figures 1a and 1c is at 230 m depth and vertical sections in Figures 1b and 1d is along 60°W.

considerably underestimates variability is to steepen the frontal structure. In this way the available potential energy as source for eddies generated by baroclinic instability is enhanced.

[17] The parameter of proportionality γ was calculated from regressions employing data or the corresponding fields from the solution of the forward model. It spans a range of values between 122 cm for the model solution and values of 434–667 cm for the climatologies and TP/ERS1 SSH variability. The correlation coefficients are of the order of 0.7. The small value for the model solution may partly be due to the fact that a large portion of the SSH variability of the model is over shallow regions where the parameterization is not defined. The value for the implementation into the adjoint is chosen as $\gamma = 200$ cm between 10°N and 50°N and $\gamma = 0$ elsewhere to exclude tropical and high-latitude regions. Tropical regions are excluded since the parameterization is based on the thermal wind relation. Low correlation coefficients in high latitudes suggest that the relation is not suitable in this region.

[18] In order to explain the effect of the parameterization, gradients of cost function parts of experiments described in section 5.2 are calculated. The two cost function parts

$$J_{SSH} = \frac{1}{N} \sum_n \frac{\left(\sigma_{SSH_n} - \sigma^{obs}_{SSH_n}\right)^2}{\epsilon^2_{d,\sigma_{SSH}}} \tag{7}$$

and

$$J_{WAO97} = \frac{1}{N} \sum_n \left(\frac{\left(T_n - T^{obs}_n\right)^2}{\epsilon^2_{d,T}} + \frac{\left(S_n - S^{obs}_n\right)^2}{\epsilon^2_{d,S}} \right) \tag{8}$$

measure the difference of the modeled rms SSH variability σ_{SSH} to the data and the difference of modeled annual mean temperature and salinity to the values of the WOA97 data, respectively. The grid point index is n, and N is the number of grid points of the model. Horizontal and vertical cross sections through cost function gradients with respect to the temperature initial condition T_o are shown in Figure 1.

Although there are marked differences between the patterns, both indicate the same characteristic errors of the model which has a northward displaced Gulf Stream with too low variability and almost no Azores Current with the associated variability. The general features of $\partial J_{SSH}/\partial T_o$ confirm the supposition made above; locations of underestimated SSH variability are distinguished by spatial gradients in the proposed temperature change. Spatial structures of the gradients of either part are consistent in suggesting warmer water south and colder water north of the Gulf Stream position. The vertical structure of both gradients share some similar features. The scheme therefore provides a method for the vertical extrapolation of SSH data. The precise position of the Gulf Stream is difficult to constitute from $\partial J_{WOA97}/\partial T_o$ while the gradient of J_{SSH} contains spatial gradient information that clearly marks the position. In the same way, the signature of the Azores front clearly derives from the associated variability whereas the climatology is too smooth to allow for any horizontal structure of the gradient in this region.

5. Assimilation Experiments

[19] The parameterization (6) is based only on horizontal and vertical gradients of the mean density. There is no constraint on absolute density values and the distribution among temperature and salinity is provided by assimilating rms SSH variability. It follows that an application of the scheme for the estimation of initial conditions for temperature and salinity will result in a large subspace of equivalent solutions. In other words, the solution will be substantially underdetermined. In the subsequent sections two ways are presented to handle this problem. One is the inclusion of a priori information for the temperature and salinity initial conditions and a second is to add climatological data of temperature and salinity. Different strategies concerning the set of the included cost function terms are pursued. The cost function is defined as a sum of quadratic parts

$$
\begin{aligned}
J &= J_T^d + J_S^d + J_{\sigma_{SSH}}^d + J_{SST}^d + J_T^f + J_S^f + J_T^i + J_S^i \\
&= \frac{1}{N}\left(\sum_n \frac{\left(T_n - T_n^{obs}\right)^2}{\epsilon_{d,T}^2} + \sum_n \frac{\left(S_n - S_n^{obs}\right)^2}{\epsilon_{d,S}^2} \right. \\
&\quad + \sum_n \frac{\left(\sigma_{SSH_n} - \sigma_{SSH_n^{obs}}\right)^2}{\epsilon_{d,\sigma_{SSH}}^2} + \sum_n \frac{\left(SST_n - SST_n^{obs}\right)^2}{\epsilon_{d,SST}^2} \\
&\quad + \sum_n \frac{\left(hfl_n - hfl_n^o\right)^2}{\epsilon_{f,T}^2} + \sum_n \frac{\left(sfl_n - sfl_n^o\right)^2}{\epsilon_{f,S}^2} \\
&\quad \left. + \sum_n \frac{\left(T_n(t=0) - T_n^o\right)^2}{\epsilon_{i,T}^2} + \sum_n \frac{\left(S_n(t=0) - S_n^o\right)^2}{\epsilon_{i,S}^2} \right),
\end{aligned}
$$

where N is total number of grid points of the model. The order of the *J*-terms correspond to the order of the sums below. The term for annual or climatological means of observational data are labeled with *d* and *i*, *f* denotes the a priori information term for initial conditions and the surface heat (hfl), and salt flux (sfl), respectively. The notation corresponds to the naming of the weights $\epsilon_{\beta,\alpha}$ introduced in Appendix A. The configuration of all performed experiments is listed in Table 1. The iterations are started with the same parameter set as the control run which is the year after a 20-year ''spin-up'' from the state of rest.

Table 1. Configuration of the Performed Experiments[a]

Experiment	J_T^d	J_S^d	$J_{\sigma_{SSH}}^d$	J_{SST}^d	J_T^f	J_S^f	J_T^i	J_S^i
SST_SSH_O			*	*	*	*	*	*
SST_SSH			*	*	*	*		
CLIM_SSH	*	*	*					
CLIM	*	*						

[a] $J_{\sigma_{SSH}}^d$, J_{SST}^d, J_T^d, and J_S^d are the cost function contributions of SSH variance, sea surface temperature, and of WOA97 temperature and salinity data, respectively. J_T^i, J_S^i, J_T^f, and J_S^f are the terms for a priori information of temperature and salinity initial conditions and of the corresponding fluxes, respectively.

5.1. Including A Priori Information

[20] The need for an additional source of temperature and salinity information in connection with the parameterization was stressed in section 4. In the experiment SST_SSH_O, a priori information of the temperature and salinity initial conditions ensures that the density information is not arbitrarily distributed among temperature and salinity corrections. The cost function consists of six terms which include the a priori information of the fluxes and the initial condition J_T^f, J_S^f, J_T^i, and J_S^i, respectively. The data terms are $J_{\sigma_{SSH}}^d$ and J_{SST}^d. The estimated parameters are the initial conditions for temperature and salinity and the corresponding surface fluxes. Only a brief description of the results is presented to give insight into the reasons for the configuration chosen in the following section. Figure 2 depicts the annual mean SSH from the control run and the final iteration together with data from *Singh and Kelly* [1997] who estimated mean SSH from a combination of hydrographic and altimeter data. The mean front of the control run is displaced at around 60°W to the north and is shifted at around 42°W to the east and it is noticeably weaker than the observations suggest. While the final iteration resembles more the control run than the data of *Singh and Kelly* [1997], the solution is nevertheless improved. This supports the assumption made in the introduction that it may be possible to retrieve some information on the mean state by assimilating variability.

[21] A similar experiment (SST_SSH) employing the same data sets without including the a priori information was performed. The parameter set encompasses heat flux and temperature initial conditions only. The mean SSH pattern shown in Figure 3 is in better agreement with the data of *Singh and Kelly* [1997] shown in Figure 2c. The Gulf Stream position is remarkable similar to the one that can be inferred from the gradient shown in Figure 1. A particular feature of this experiment is an almost correct Gulf Stream separation east of Cape Hatteras which was found to remain stable for more than 2 years as the model was integrated for 2 additional years. This suggests that the a priori information of the initial condition is very efficient in keeping the solution close to the reference run.

5.2. Including WOA97 Data

[22] In the experiment CLIM_SSH the WOA97 data were directly included into the cost function to constrain the

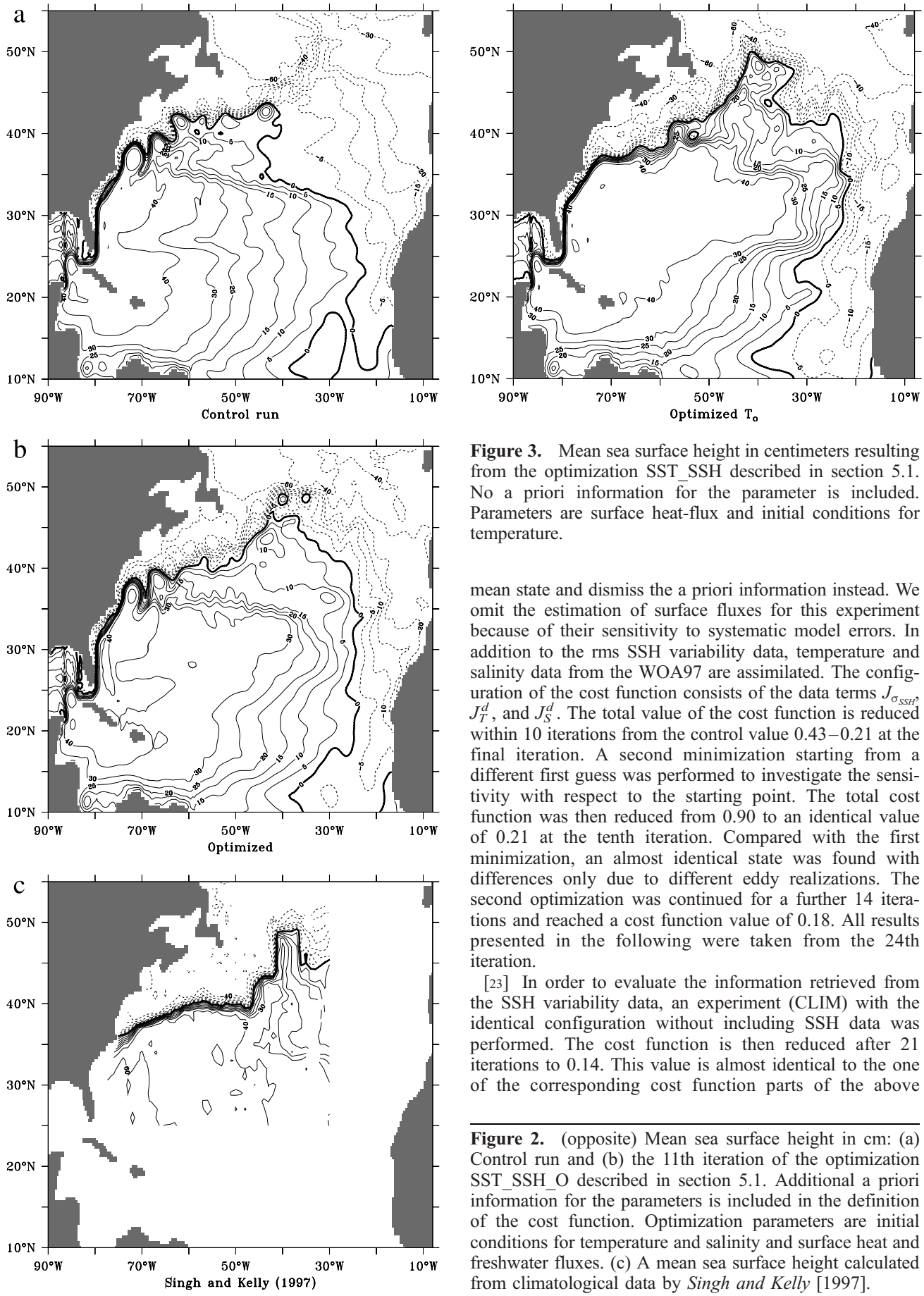

Figure 3. Mean sea surface height in centimeters resulting from the optimization SST_SSH described in section 5.1. No a priori information for the parameter is included. Parameters are surface heat-flux and initial conditions for temperature.

mean state and dismiss the a priori information instead. We omit the estimation of surface fluxes for this experiment because of their sensitivity to systematic model errors. In addition to the rms SSH variability data, temperature and salinity data from the WOA97 are assimilated. The configuration of the cost function consists of the data terms $J_{\sigma_{SSH}}$, J_T^d, and J_S^d. The total value of the cost function is reduced within 10 iterations from the control value 0.43–0.21 at the final iteration. A second minimization starting from a different first guess was performed to investigate the sensitivity with respect to the starting point. The total cost function was then reduced from 0.90 to an identical value of 0.21 at the tenth iteration. Compared with the first minimization, an almost identical state was found with differences only due to different eddy realizations. The second optimization was continued for a further 14 iterations and reached a cost function value of 0.18. All results presented in the following were taken from the 24th iteration.

[23] In order to evaluate the information retrieved from the SSH variability data, an experiment (CLIM) with the identical configuration without including SSH data was performed. The cost function is then reduced after 21 iterations to 0.14. This value is almost identical to the one of the corresponding cost function parts of the above

Figure 2. (opposite) Mean sea surface height in cm: (a) Control run and (b) the 11th iteration of the optimization SST_SSH_O described in section 5.1. Additional a priori information for the parameters is included in the definition of the cost function. Optimization parameters are initial conditions for temperature and salinity and surface heat and freshwater fluxes. (c) A mean sea surface height calculated from climatological data by *Singh and Kelly* [1997].

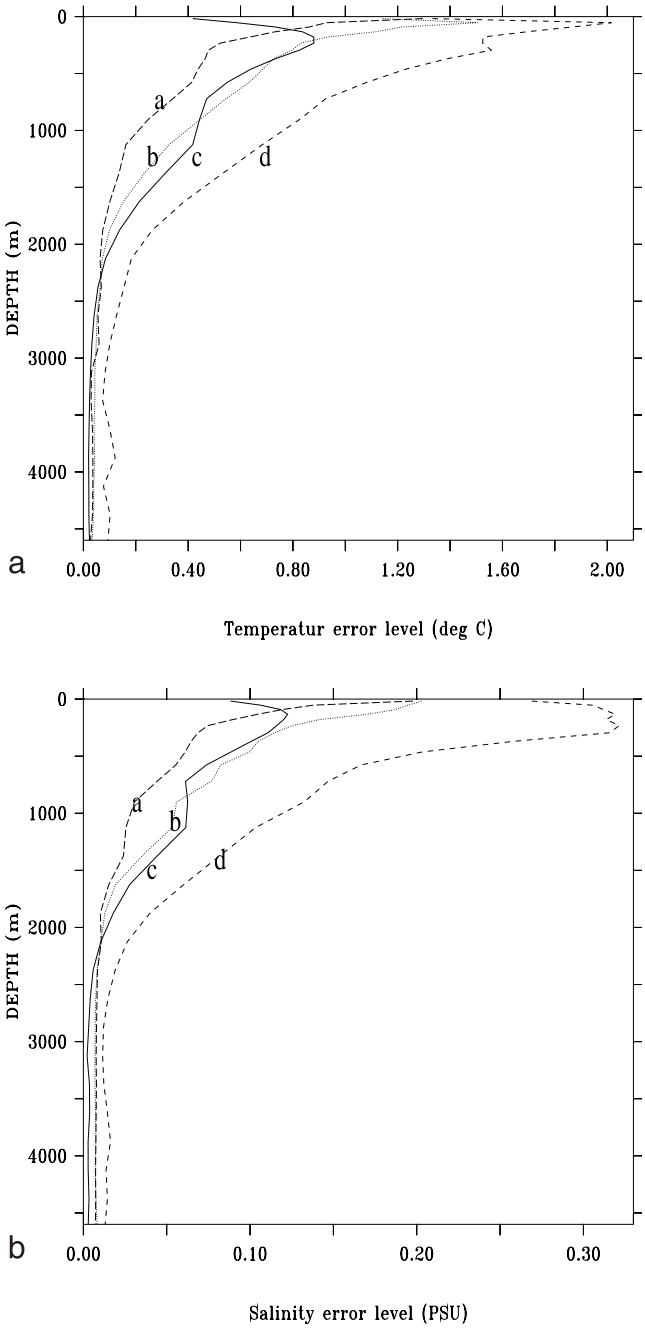

Figure 4. Posterior error profiles calculated from the rms difference with temperature and salinity fields of the WAO97 climatology. (d) Control, (c) assimilation run CLIM_SSH, (b) twice the ensemble rms variance, (a) and the rms difference between the SAC and the WOA97 climatologies from Figure 13.

described experiment that includes additionally the rms SSH variability term which accounts for 0.067 of the 0.21. Identical hydrographic cost function parts indicate that changes introduced by the SSH information are independent of, or consistent with the adjustments related to the hydrographic data.

[24] The effect of assimilation in the experiment CLIM_SSH is assessed by profiles of posterior rms errors depicted in Figure 4. Except for the near surface region, the profiles are generally in the order of twice the ensemble error variance corresponding to a 95% level. It is not clear whether an rms error in the order of the a priori estimates could actually by reached, particularly since the eddy variability is markedly enhanced (see the following) and signatures of the eddies are still present in the annual mean values. The failure in the surface region results from inconsistent surface fluxes, which were not optimized. The inclusion of rms SSH variability data does not affect noticeably the error profiles in the assimilation run (compare the profiles in Figures 4e and 4f). This supports the assumption that information introduced by the assimilation of rms SSH variability is consistent with the WOA97 data. A slow return to the state of the control is documented by an increase of the rms error for the second year (the profile in Figure 4d).

[25] Figures 5a and 6a show the temperature and salinity differences between the control run and the assimilated data in 580 m depth. The largest temperature and salinity

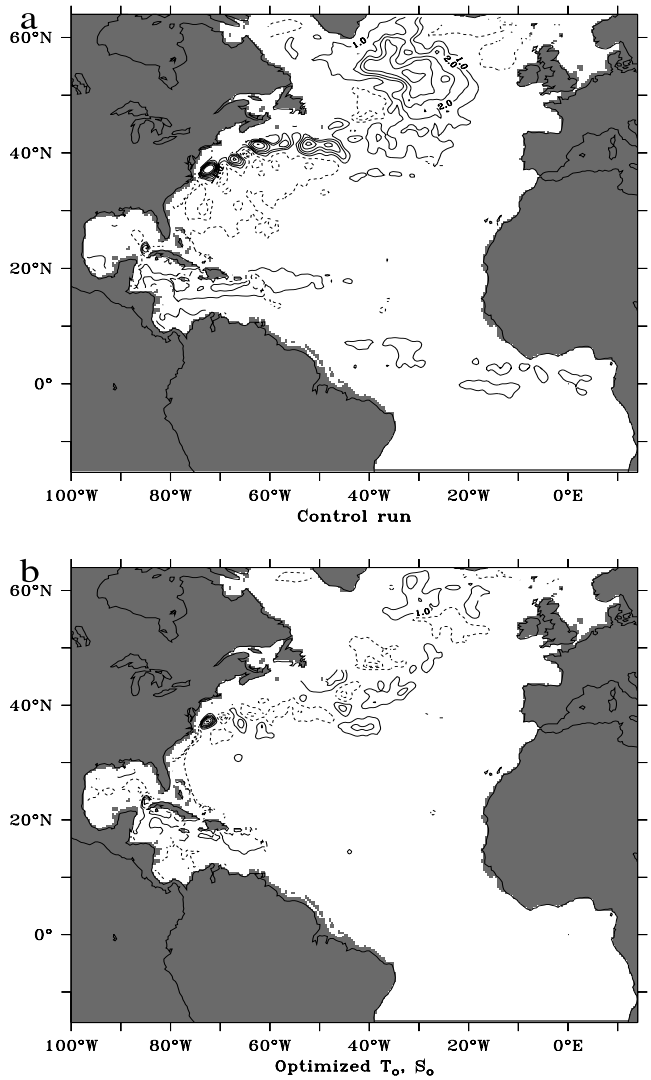

Figure 5. Temperature difference in °C in 580 m: (a) Control run-WOA97 data and (b) experiment CLIM_SSH − WOA97 data (ci = 1°C).

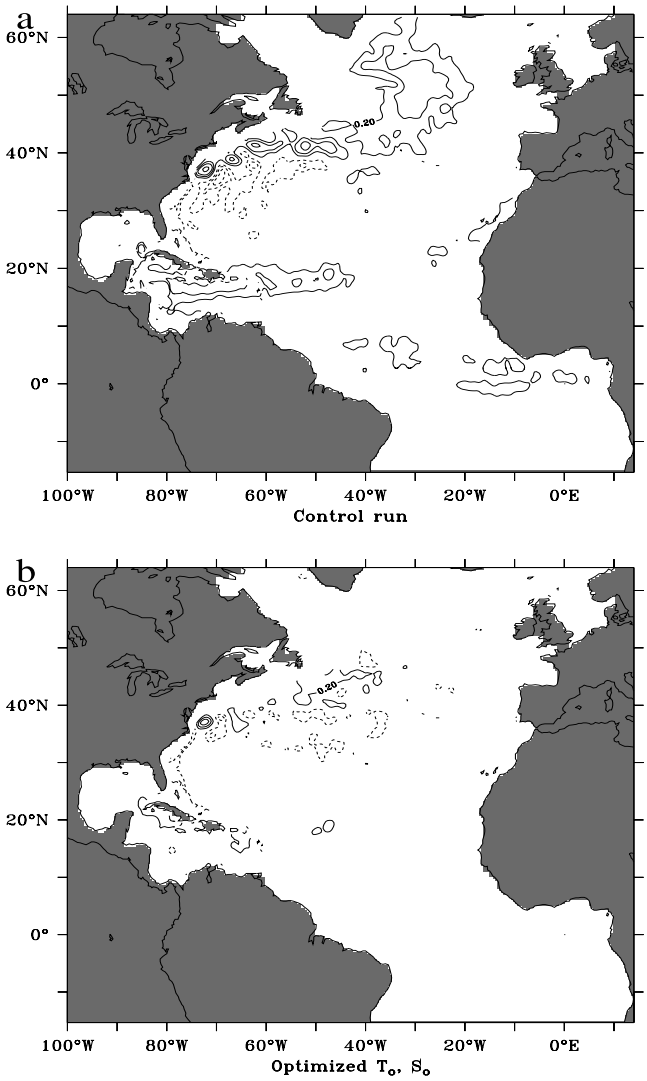

Figure 6. Salinity difference in 580 m: (a) Control run-WOA97 data and (b) experiment CLIM_SSH − WOA97 data (ci = 0.2 PSU).

anomalies are in the Sargasso Sea and originate from the northward displaced Gulf Stream. The positive temperature and salinity anomalies in the Irminger Sea reflect a North Atlantic Current (NAC) that is located too far west and leads into the Irminger Sea. Smaller deviations are visible in the Caribbean Sea and near the equator. The main source for the error in the assimilation experiment CLIM_SSH, displayed in Figures 5b and 6b, is caused by spurious eddies which are still present in the mean fields. The largest differences remain in the regions of high eddy kinetic energy, particularly in the region of Gulf Stream and the NAC. Significant differences also occur east of Grand Banks and in the Caribbean Sea. Below 1000 m (not shown), differences remain after optimization due to the eddy-like spots present within WOA97 data. The resulting mean state still has substantial deficiencies as will be shown in the following. Since the remaining error is to some extent caused by the irreducible part emerging from the eddy effects, a further reduction is difficult to achieve.

[26] The rms SSH variability error is reduced from 7.2 cm to 4.8 cm. Figure 7 shows the rms SSH variability from the control and the assimilation CLIM_SSH together with the observational data. The maximum of the variability of the control is displaced northward and overall too low with a maximum around 47°N. By assimilation of rms SSH variability and WOA97 data (Figure 7c), the erroneous maximum vanished and the mean position and amplitude of maximal variability is fairly well matched, It does extends further to the north around 55°W, and the northward extension at 42°W is not captured. The turnoff of the Azores Current is visible by increased variability. The scales of eddies are clearly too large in comparison with the observations which may be explained by too low a resolution. The level of SSH variability in the Gulf Stream region is also enhanced to a realistic magnitude by assimilating only the WOA97 data, but its position and the maximum around 47°N is not changed.

[27] The mean SSH of the experiment CLIM_SSH is illustrated in Figure 8b. It supports the findings from Figure 7. The position and amplitude around 60°W matches the data of *Singh and Kelly* [1997] (see also Figure 2) with a slightly weaker front. However, the front at 42°W is not present in Figure 8b, although it may be seen in the estimated initial conditions, indicating a dynamical deficit of the model. The amplitude of the stationary anticyclone east of Cape Hatteras is reduced together with the disappearance of the front resembling a wrong turnoff position of the Azores Current. The mean SSH in Figure 8a results from experiment CLIM and represents a somewhat intermediate state between the control state in Figure 2a and data in Figure 8b. The Gulf Stream front is stronger, but the position is nearly unchanged in comparison to Figure 2a. The pattern in the Azores region resembles the one of Figure 8b, but the strength of the front is very weak.

[28] In order to investigate whether the solution CLIM_SSH is a new equilibrium state, the integration is continued further. Within the following 2 years of integration the state returns toward the pattern of the control run. The mean front starts continuously to split into a northward displaced and a southern front visible in Figure 2a. The return is documented in Figure 9, which shows a meridional temperature section in the Gulf Stream region. Cold water inserted north of the Gulf Stream is rapidly removed, whereas the mean frontal position only slowly returns to the position of the control run. As a consequence of this rapid removal, temperature corrections of the initial condition are overestimated. For the same region as displayed in the figure, temperatures in January are about 1.5°C too low at 44°N in comparison with the monthly mean value of the WOA97 data.

[29] As visible from the near surface velocities of experiment CLIMSSH in Figure 10a, the Azores Current of the control run is only represented as a markedly southward shifted band branching east of Cape Hatteras from the Gulf Stream. Assimilation shifts the band to the observed position at 34°N [*Gould*, 1985], and the current originates from the separation of the Gulf Stream into the North Atlantic Current (NAC) and the Azores Current (Figure 10b), as suggested by *Sy* [1988]. The erroneous flow of the NAC towards the Irminger Sea visible in Figure 10a is corrected and the transport follows after assimilation the realistic

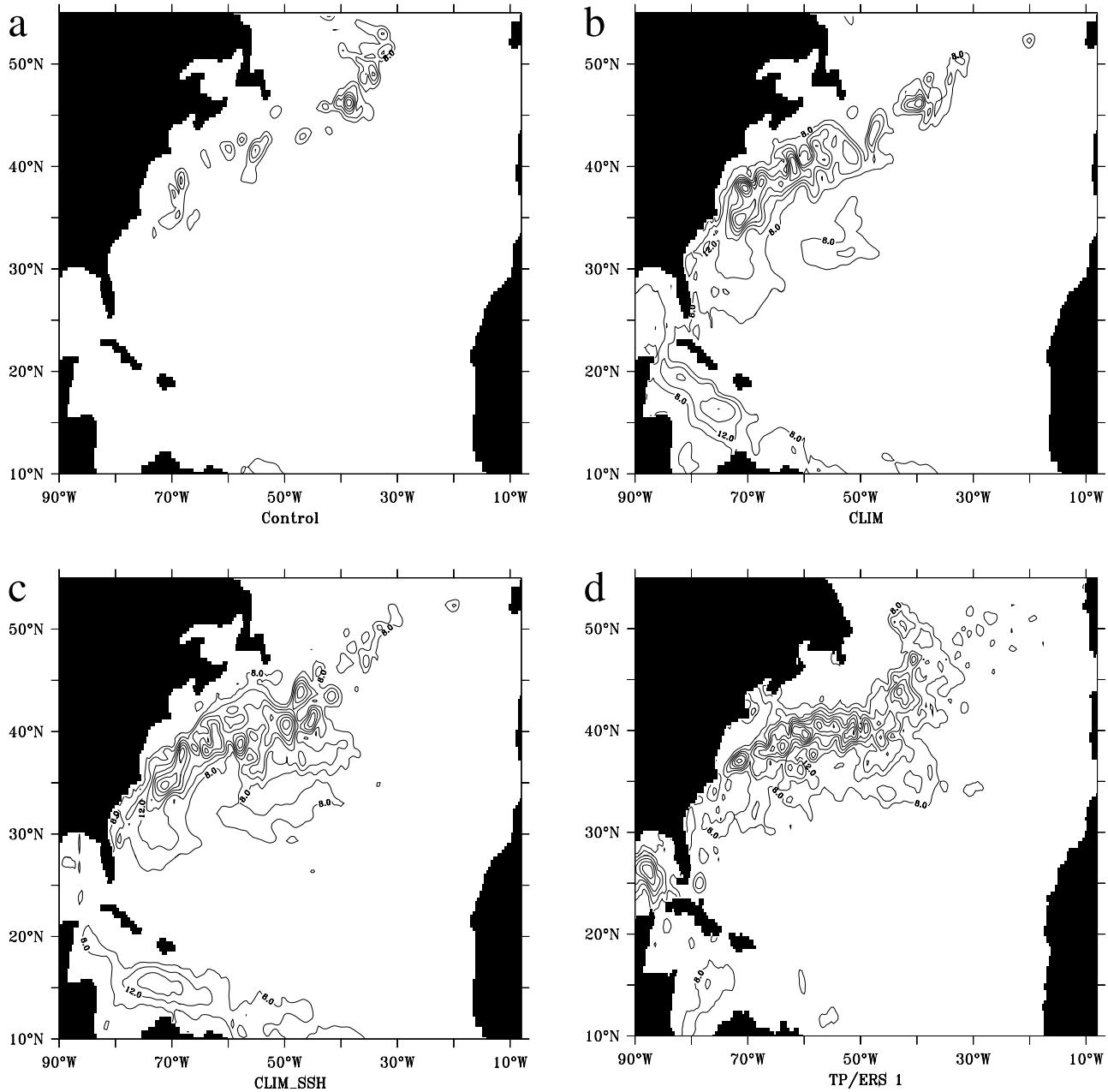

Figure 7. RMS SSH variability in centimeters. (a) Control run. Figures 7b and 7c are from the assimilation experiments CLIM and CLIM_SSH of section 5.2, respectively. The SSH data is depicted in Figure 7d.

route towards the Norwegian Sea, although it deflects east of the Rockall Plateau to the northwest.

[30] The position of the Azores front is difficult to identify in the control from the potential density section averaged between 35°*W*–30°*W* as illustrated in Figure 11, whereas in the CLIM_SSH run the frontal structure is even more pronounced than in the WOA97 data. Likewise, the position is shifted slightly to the north, indicating that the front is mainly established by information from the altimeter data.

[31] The amplification of the EKE level shown in Figure 12 from values less than 4 $cm^2\ s^{-2}$ to values up to 20 $cm^2\ s^{-2}$ in average accompanies the intensification of the Azores Current. This is still much too low compared with more than 150 $cm^2\ s^{-2}$ as calculated from cross-track geostrophic velocity of TOPEX/POSEIDON [*Stammer and Böning*, 1996] or from drifter data [*Brügge*, 1995]. Some iterations show values up to 100 $cm^2\ s^{-1}$. It should be noted that the associated SSH variability is then found to be higher than the values from TP/ERS1. Values over 100 $cm^2\ s^{-2}$ are thus not consistent with the assimilated SSH variability from mapped TP/ERS1 data. The interpolation of track data generally underestimates the amplitude of the real signal. Moreover, EKE and SSH variability are related through a length scale, which is too large in the model. The associated velocities are thus too low, and a simulation consistent with both SSH variability and EKE is not possible. There is nearly no improvement through the assimilation of only climatological data and a slight enhancement is visible in

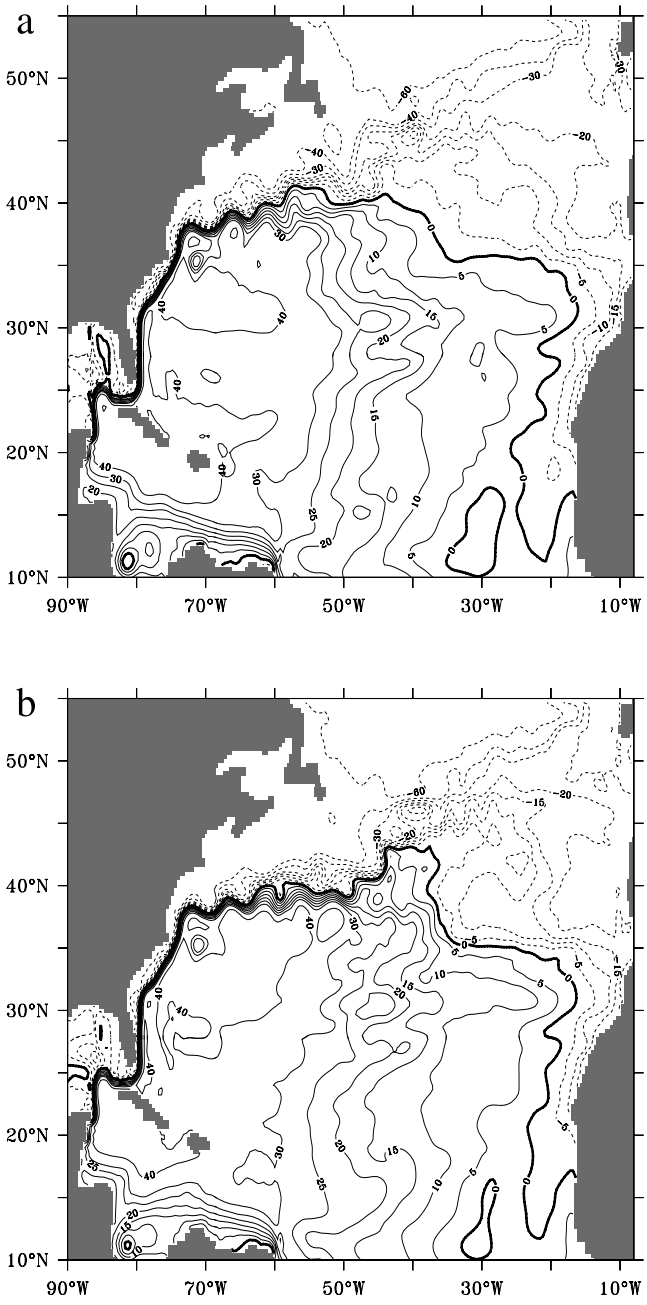

Figure 8. Mean sea surface height in centimeters from the experiments (a) CLIM and (b) CLIM_SSH of section 5.2.

Figure 12 only north and south of the current position for the experiment CLIM. The reason for this is, as indicated in Figure 11, a too weak frontal slope in the climatological data due to smoothing.

[32] The deep circulation is affected by the introduction of water masses through the initial conditions. The meridional overturning stream function remains mostly unchanged north of 40°N where the overturning is mainly controlled by the northern boundary condition [*Döscher et al.*, 1994]. It increases to unrealistic values of about 30 Sv north of the equator with a maximum at about 13°N. The strength of the overturning continuously increases with the number of iterations. An increased sinking between 15°N and 20°N is limited to the region of the Caribbean Sea and north east of the Antilles where larger differences to the WOA97 data occur. In spite of this difference, continuously denser water is introduced between 600 m and 1000 m depth in this region during the optimization. It is not quite clear if the adjoint variables in this region are affected by remote model-data differences or if approximations made within this method are responsible for a wrong estimation of the gradient in this area. The steep topography in this region, representing the Island chain of the Antilles, is different in the forward and the adjoint model. Land may separate in the forward model two ocean parts that are not separated in the adjoint. The horizontal mixing between those parts might be possible in the adjoint. However, a similar overturning cell north of the equator was also observed by *Ayoub et al.* [2001] from an assimilation experiment with a 1° North Atlantic model. The meridional heat transport which is closely related to the overturning strength [*Böning et al.*, 1996] also nearly doubled in the area around 15°N. The quite small difference to the WOA97 data in terms of the contribution to the cost function (differences due to eddy signatures at the same level in the Gulf Stream region or due to insufficient smoothing of the WOA97 data are much larger) has important dynamical consequences. The overturning and heat transport have returned in the following year back to the values of the control. Although the unrealistic transport values could be related to deviation from WOA97 data, the results demonstrate a poor skill for determining these quantities from assimilation experiments when quasi-stationarity is not guaranteed.

6. Conclusion

[33] Our intention was to provide a framework for state estimations with high-resolution ocean models. The princi-

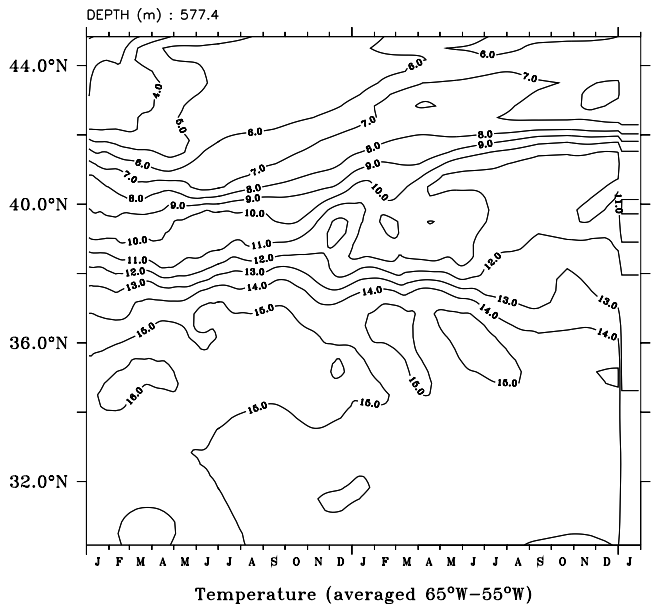

Figure 9. Time series showing the slow return of the Gulf Stream front position to the location of the reference run. The series starts after insertion of optimized initial conditions for temperature and salinity of experiment CLIM_SSH. The temperature in 550 m depth is averaged from 65°W to 55°W. Mean values of the control run are added in January after the second year to mark the difference to the control run.

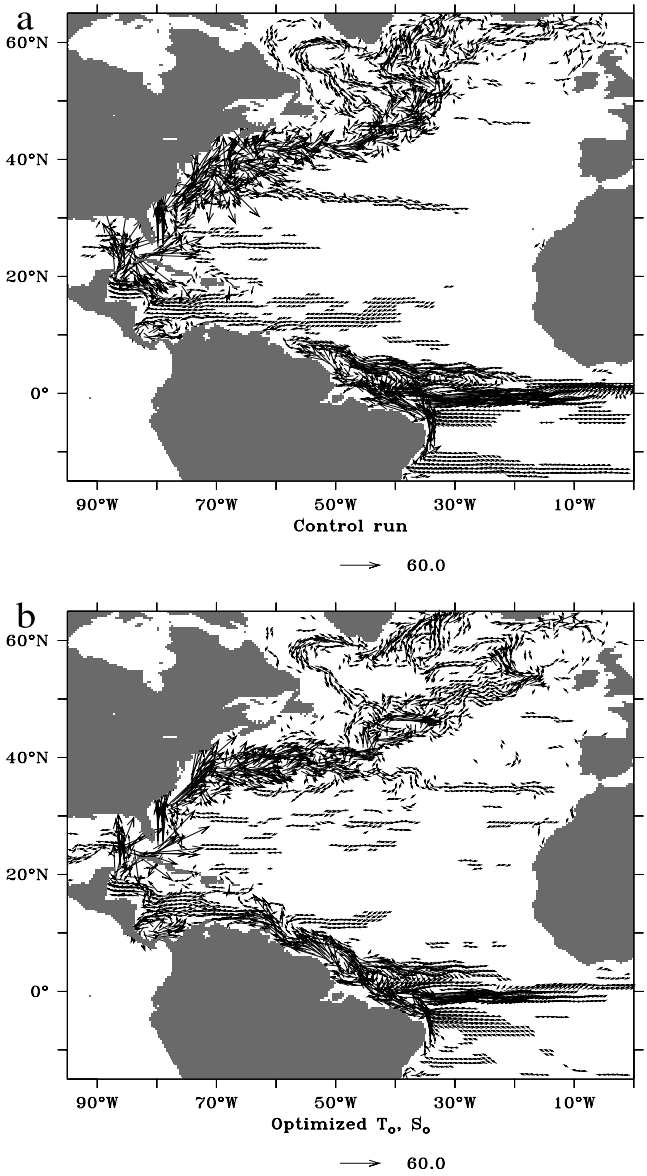

Figure 10. Annual mean velocity at 90 m in centimeters per second. (a) Control and (b) from the assimilation run CLIM_SSH.

pal feasibility of the method for improving the climatological state of eddy-resolving models was demonstrated by assimilating SSH variability and climatological data. However, it was not possible to find a new stable equilibrium state by estimating the initial conditions for temperature and salinity. On annual periods the mean state is markedly improved in comparison with the reference state but not fully consistent with the assimilated data. Furthermore, the state is not in a statistical equilibrium and still subject to deficits.

[34] We have shown that the assimilation of SSH variability with a parameterization derived from baroclinic instability theory yields information that is complementary as well as consistent with the WOA97 climatology. An important aspect of this new technique is the potential to extract characteristics of mean frontal structures from variability, since this type of information is not well represented in climatological data which are usually subject to extensive smoothing. In this way, it was possible to determine aspects of the mean state with information from the SSH variability.

[35] In order to assess the success of the assimilation it is not sufficient to regard only assimilated quantities. Since the adjoint method enforces consistency with dynamics of the model, the quality of the mean state and quantities that were derived via the dynamical equations are limited by dynamical deficits or parameters of the model that were not included in the optimization. At a resolution of 1/3° eddies are only marginally represented and eddy velocities are too small, the realistic SSH variability is therefore connected with a too low level of EKE.

[36] It appears from some iterations that a marginally stable solution showing a correct Gulf Stream separation with a small basin of attraction persists for more than 1 year. The transition to the reference solution may then be induced by eddy variability or by a slow change that comes along with increased heat transport. It is thus plausible that only minor changes in the model dynamics might be sufficient to

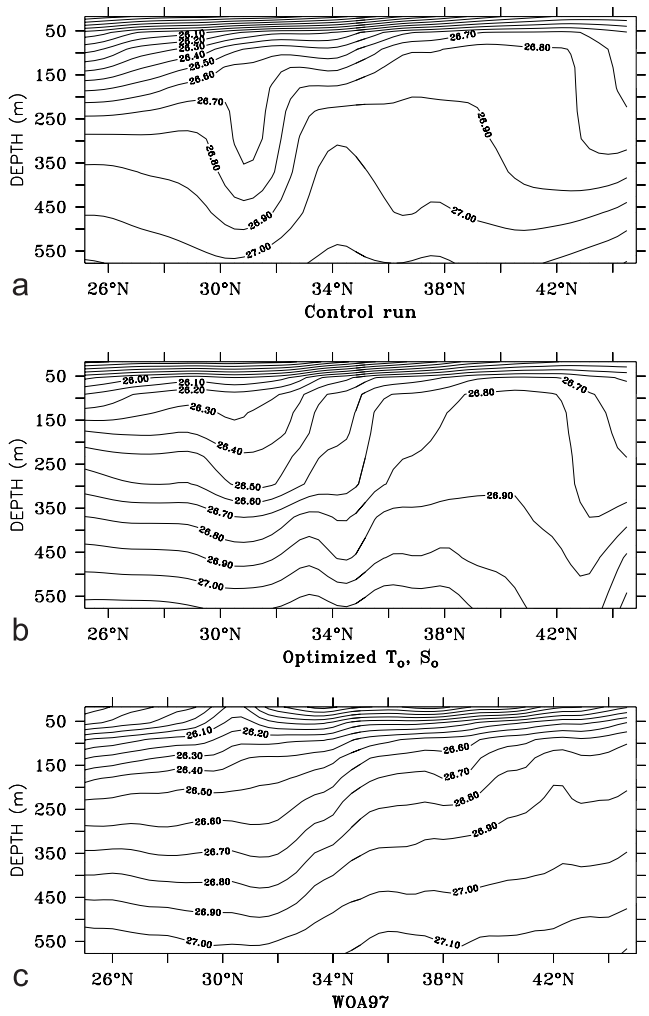

Figure 11. Sections of potential density averaged from 35°W–30°W (ci = 0.1). (upper) Control run, (middle) assimilation run CLIM_SSH, and (lower) data from *Boyer and Levitus* [1997].

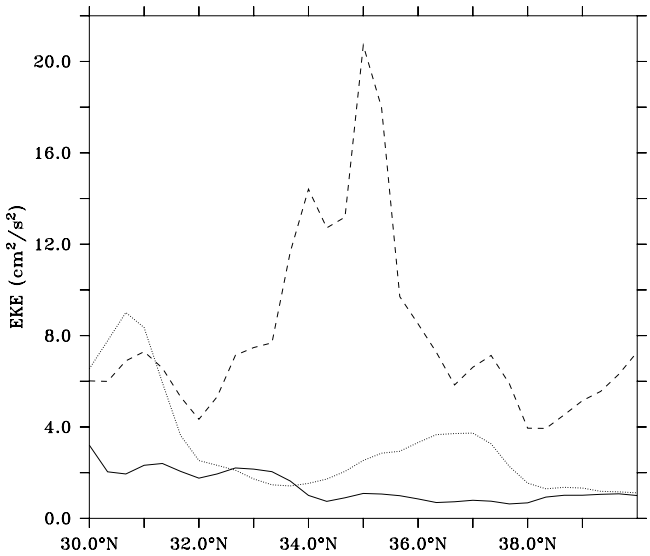

Figure 12. Near surface eddy kinetic energy averaged from 35°W to 25°W for the control run together with values from the assimilation CLIM_SSH (dashed) and CLIM (dotted).

enable a correction for at least this point. At the given resolution it seems not very likely though that a parameter setting can be found which corrects systematic errors that a great majority of this type of models share.

Appendix A: Data Sets and Error Estimates

[37] Estimations for the error covariances are given in the following for each term of the cost function. In order to calculate estimations of the covariances, an approach was followed that is similar to *Evensen* [1994] and *Evensen and van Leeuwen* [1996], who derived the forecast error covariance matrix from an ensemble of forward calculations. Presuming uncorrelated model and data errors, the error covariance can be written as a combination of the model and the data error covariance. The general assumption for the adjoint method is that the model error could be identified with the parameters or controls of the optimization problem. In other words, it is assumed that the model has no systematic errors other than those contained in explicit parameters. This assumption is clearly a limitation for the validity of the use of an adjoint method.

[38] The approximation of the forward statistical model by time averages from the solution of the high-resolution model introduces an additional source of model error. Because of the finite averaging time of 1 year, the time averages still contain signatures of the eddy field. As described in KW, the variance of these mean values provides an estimate of the statistical model error. The variance depends on the length of the averaging period and is derived from an ensemble of seven successive integrations over 1 year, after 20 years of integration. These annual mean values may be regarded as independent owing to the rapid decorrelation of the transient eddy signal. If not otherwise specified, we consider only the diagonal elements of the error covariance matrix averaged over time and horizontal directions, i.e., a number or a profile.

A1. SSH Variability

[39] Sea surface height variance is calculated from five-daily maps of merged data from TOPEX/POSEIDON and ERS1 (TP/ERS1) created by *Oschlies and Garçon* [1998] enclosing the period from October 1992 to October 1993 (see also Figure 7d). The total measurement error as given by [*Fu et al.*, 1994] is 4.7 cm for TOPEX and 5.1 cm for POSEIDON, while an overall rms difference of 3 cm to tide gauge measurements is found by [*Morris and Gill*, 1994].

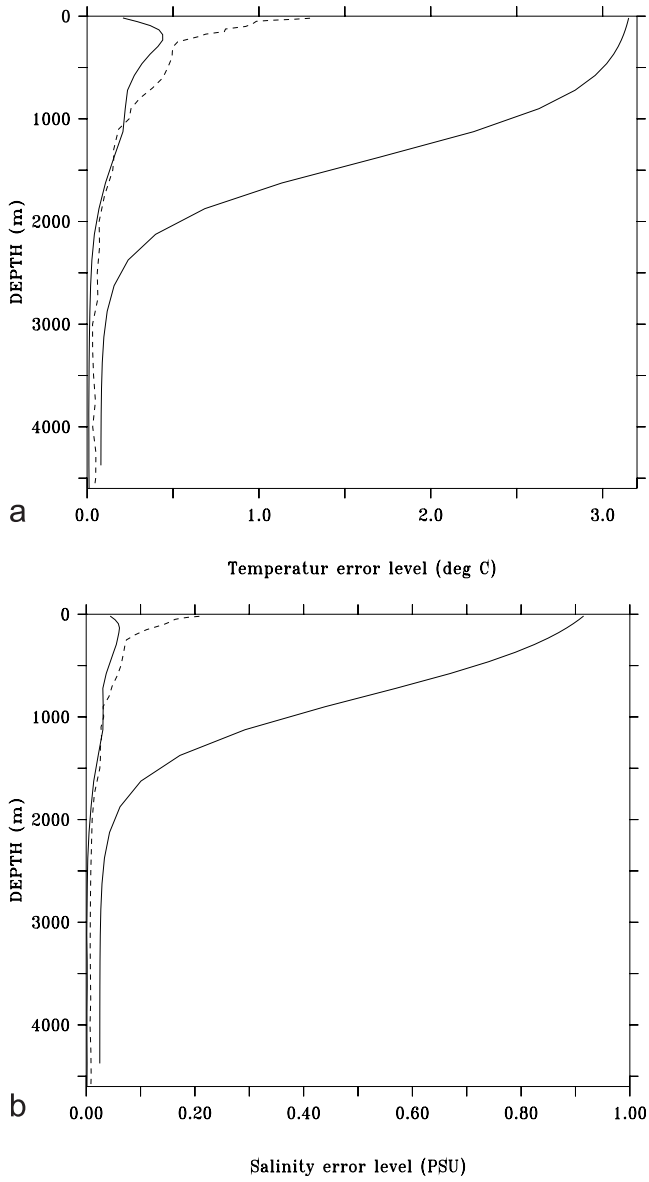

Figure 13. Square root of the horizontally averaged variance of annual mean values (thin solid) together with the averaged rms difference between WAO97 and SAC climatology (dashed). The bold profiles are the specified error functions $\epsilon_T^d(z)$ and $\epsilon_S^d(z)$ used for the error covariance. They contain estimations of the reduction in degrees of freedom due to vertical correlation within the T and S data and are therefore larger than estimations of the variances.

We have used a constant value of $\epsilon_{d,\sigma_{SSH}} = 4$ cm throughout the experiments.

A2. SST

[40] The sea surface temperature (SST) is taken from the 9 km resolution daily nighttime maps of the AVHRR Oceans Pathfinder Program [*Smith et al.*, 1996]. The mean SST is calculated from maps covering the same period as the SSH data after building monthly mean values to reduce the bias due to cloud cover. The rms difference between the gridded Pathfinder SST data and SST from a buoy database [*Podesta et al.*, 1995] is 0.97°C for the nighttime matchups [*Smith et al.*, 1996]. The error value for temperature observations is chosen as $\epsilon_{d,SST} = 1$°C.

A3. Climatological Data of Temperature and Salinity

[41] The depth-dependent rms difference of temperature and salinity values between climatologies of *Boyer and Levitus* [1997], hereafter WOA97 and *Gouretski and Jancke* [1998], hereafter SAC is depicted in Figure 13 together with values calculated from the variance of an ensemble of seven annual mean values from the model. Both approaches provide similar estimates for the error profiles except in the surface region where variability is underestimated by the model due to the restoring to monthly mean values.

[42] Vertical correlations in the temperature and salinity fields, which effectively reduce the number of independent degrees of freedom, have to be taken into consideration in particular when surface data is included in the cost function. Typical vertical correlation radii calculated from the above described ensemble are 350 m above and 500 m below 1000 m depth. Profiles that approximate the rms temperature and salinity error profiles, respectively, are multiplied by a factor that counts the number of layers within the correlation radius.

A4. Initial Conditions

[43] The first guess for the initial condition is the state after 20 years of ''spin-up.'' The error weight was approximated by the deviation of the annual mean values of the reference experiment in comparison with temperature and salinity data from the WOA97 with the additional modification to account for vertical correlations. The approximations for the error profiles of the a priori information then reads, $\epsilon_{i,T}(z) = 14$°C $\exp(-z/800$ m) and $\epsilon_{i,S}(z) = 4$ PSU $\exp(-z/800$ m), respectively.

A5. Surface Flux

[44] Weighting coefficients for the a priori parameter values of heat and freshwater fluxes estimated as restoring temperature and salinity were chosen as $\epsilon_{f,T} = 4$°C and $\epsilon_{f,S} = 0.5$ PSU. For the CME model the values correspond approximately to heat and fresh water flux values of about 32 Wm^{-2} and 1 m yr^{-1}, respectively.

[45] **Acknowledgments.** The work was supported by the Bundesministerium für Forschung und Technologie as part of the German WOCE.

References

Ayoub, N., D. Stammer, and C. Wunsch, Estimating the North Atlantic circulation with nesting and open boundary conditions using an adjoint model, *ECCO Rep. 10*, Scripps. Inst. of Oceanogr., La Jolla, Calif., 2001.

Böning, C. W., Large-scale transport processes in high-resolution circulation models, in *The Warmwatersphere of the North Atlantic Ocean*, pp. 91–128, Gebrüder Bornträger, Berlin, 1996.

Böning, C. W., F. O. Bryan, W. R. Holland, and R. Döscher, Deep-water formation and meridional overturning in a high-resolution model of the North Atlantic, *J. Phys. Oceanogr.*, *26*, 1142–1164, 1996.

Boyer, T. P., and S. Levitus, Objective analyses of temperature and salinity for the world ocean on a 1/4 degree grid, *NOAA Atlas NESDIS 11*, U.S. Gov. Print. Off., Washington, D. C., 1997.

Brügge, B., Near surface mean circulation and eddy kinetic energy in the central North Atlantic from drifter data, *J. Geophys. Res.*, *100*, 20,543–20,554, 1995.

Bryan, F. O., and W. R. Holland, A high-resolution simulation of wind- and thermohaline-driven circulation in the North Atlantic Ocean, in *Parametrizations of Small Scale Processes, Proceedings of the Aha Huliko a Hawaiian Winter Workshop*, pp. 99–115, edited by P. Müller and D. Henderson, Univ. of Hawaii, Honolulu, 1989.

Cooper, M., and K. Haines, Altimetric assimilation with water property conservation, *J. Geophys. Res.*, *101*, 1059–1077, 1996.

Dijkstra, H. A., and M. J. Molemaker, Imperfections of the North Atlantic wind-driven ocean circulation: Continental geometry and windstress shape, *J. Mar. Sci.*, *57*, 1–28, 1999.

Döscher, R. C., C. W. Böning, and P. Herrman, Response of circulation and heat transport in the North Atlantic to changes in forcing in northern latitudes: A model study, *J. Phys. Oceanogr.*, *24*, 2306–2320, 1994.

DYNAMO Group, *DYNAMO Dynamics of North Atlantic Models: Simulation and assimilation with high resolution models*, *Rep. 294*, Univ. Kiel, Kiel, Germany, 1997.

Evensen, G., Sequential data assimilation with a nonlinear quasigeostrophic model using Monte Carlo methods to forecast error statistics, *J. Geophys. Res.*, *99*, 10,143–10,162, 1994.

Evensen, G., and P. J. van Leeuwen, Assimilation of Geosat altimeter data for the Agulhas Current using the ensemble Kalman filter with a quasigeostrophic model, *Mon. Weather Rev.*, *124*, 85–96, 1996.

Fu, L.-L., E. J. Christensen, C. A. Yamarone, M. Lefebvre, Y. Ménard, M. Dorrer, and P. Escudier, TOPEX/POSEIDON mission overview, *J. Geophys. Res.*, *99*, 24,369–24,381, 1994.

Gavart, M., and P. De Mey, Isopycnal EOFs in the Azores Current region: A statistical tool for dynamical analysis and data assimilation, *J. Phys. Oceanogr.*, *27*, 2146–2157, 1997.

Giering, R., and T. Kaminski, Recipes for adjoint code construction, *Trans. Math. Software*, *24*, 437–474, 1998.

Gilbert, J. C., and C. Lemaréchal, Some numerical experiments with variable-storage Quasi-Newton algorithms, *Math. Program.*, *45*, 407–435, 1989.

Gould, W. J., Physical oceanography of the Azores front, *Progr. Oceanogr.*, *14*, 167–190, 1985.

Gouretski, V., and K. Jancke, A new world ocean climatology: Objective analysis on neutral surfaces, *WHP-SAC Tech. Rep. 3*, *WOCE Rep., 256/17*, 1998.

Green, J. S. A., Transfer properties of the large-scale eddies and the general circulation of the atmosphere, *Q. J. R. Meteorol. Soc.*, *96*, 157–417, 1970.

Han, Y.-J., A numerical world ocean general circulation model, II, A baroclinic experiment, *Dyn. Atmos. Oceanogr.*, *8*, 141–172, 1984.

Hellerman, S., and M. Rosenstein, Normal monthly windstress over the world ocean with error estimates, *J. Phys. Oceanogr.*, *13*, 1093–1104, 1983.

Kazantsev, E., Local Lyapunov exponents of the quasi-geostrophic ocean dynamics, *Appl. Math. Comput.*, *104*, 217–257, 1999.

Kazantsev, E., J. Sommeria, and J. Verron, Subgrid-scale parameterization by statistical mechanics in a barotropic ocean model, *J. Phys. Oceanogr.*, *28*, 1017–1042, 1998.

Killworth, P. D., C. Dietrich, C. L. Provost, A. Oschlies, and J. Willebrand, Assimilation of altimetric data and mean sea surface height into an eddy-permitting model of the North Atlanic, *Progr. Oceanogr.*, *48*, 313–335, 2001.

Köhl, A., and J. Willebrand, An adjoint method for the assimilation of statistical characteristics into eddy-resolving ocean models, *Tellus, Ser. A*, *54*, 406–425, 2002.

Krauss, W., and R. H. Käse, Mean circulation and eddy kinetic energy in the eastern North Atlantic, *J. Geophys. Res.*, *89*, 3407–3415, 1984.

Le Dimet, F.-X., and O. Talagrand, Variational algorithms for analysis and assimilation of meteorological observations: Theoretical aspects, *Tellus, Ser. A*, *38A*, 97–110, 1986.

Levitus, S., Climatological atlas of the world ocean, Tech. Pap., 173 pp., Natl. Ocean. Atmos. Admin., Silver Spring, Md., 1982.

Morris, C., and S. Gill, Evaluation of the TOPEX/POSEIDON altimeter system over great lakes, *J. Geophys. Res.*, *99*, 24,527–24,539, 1994.

Morrow, R., and P. De Mey, Adjoint assimilation of atlimetric, surface drifter, and hydrographic data in a quasigeostrophic model of the Azores Current, *J. Geophys. Res.*, *100*, 25,007–25,025, 1995.

Oschlies, A., and V. Garçon, Eddy induced enhancement of primary production in a model of the North Atlantic Ocean, *Nature*, *394*, 266–269, 1998.

Oschlies, A., and J. Willebrand, Assimilation of Geosat altimeter data into an eddy-resolving primitive equation model of the North Atlantic Ocean, *J. Geophys. Res.*, *101*, 14,175–14,190, 1996.

Pacanowski, R., K. Dixson, and A. Rosati, The GFDL modular ocean model users guide, Tech. Rep., Geophy. Fluid Dyn. Lab., Ocean Group, Princeton Univ., Princeton, N. J., 1993.

Podesta, G. P., S. Shenoi, J. W. Brown, and R. H. Evans, AVHRR Pathfinder Oceans Matchup Database 1985–1993 (Version 18), 33 pp., Rosenstiel Sch. of Mar. and Atmos. Sci., Univ. of Miami, Coral Gables, Fla., 1995.

Richardson, P. L., Eddy kinetic energy in the North Atlantic from surface drifters, *J. Phys. Oceanogr.*, *88*, 4355–4367, 1983.

Schröter, J., U. Seiler, and M. Wenzel, Variational assimilation of Geosat data into an eddy resolving model of the Gulf Stream extension area, *J. Phys. Oceanogr.*, *23*, 925–953, 1993.

Singh, S., and K. A. Kelly, Monthly maps of sea surface hight in the North Atlantic and zonal indices for the Gulf Stream using TOPEX/Poseidon altimeter data, *Rep. WHOI-97-06*, 50 pp., Woods Hole Oceanogr. Inst., Woods Hole, Mass., 1997.

Sirkes, Z., and E. Tziperman, Finite difference of adjoint or adjoint of finite difference?, *Mon. Weather Rev.*, *125*, 3373–3378, 1997.

Smith, E., J. Vazquez, A. Tran, and R. Sumagaysay, Satellite-derived sea surface temperature data available form the NOAA/NASA Pathfinder program, *Eos. Trans. AGU Electron. Suppl.*, 1996. (Available as http://www.agu.org/eos_elec/95274e.html)

Stammer, D., Global characteristics of ocean variability estimated from regional TOPEX/POSEIDON altimeter measurements, *J. Phys. Oceanogr.*, *27*, 1743–1768, 1997.

Stammer, D., and C. W. Böning, Generation and distribution of mesoscale eddies, in *The Warmwatersphere of the North Atlantic Ocean*, pp. 159–194, Gebrüder Bornträger, Berlin, 1996.

Stone, P. H., A simplified radiative-dynamical model for the static stability of rotating atmospheres, *J. Atmos. Sci.*, *29*, 405–418, 1972.

Sy, A., Investigation of large scale circulation patterns in the central North Atlantic: the North Atlantic Current, the Azores Current, and the Mediterranean Water plume in the area of the Mid-Atlantic Ridge, *Deep-Sea Res.*, *35*, 383–413, 1988.

Treguier, A. M., I. Held, and V. Larichev, Parametrization of quasigeostrophic eddies in primitive equation ocean models, *J. Phys. Oceanogr.*, *27*, 567–580, 1997.

A. Köhl, Scripps Institution of Oceanography, 8605 La Jolla Shores Dr., La Jolla, CA 92093-0230, USA. (akoehl@ucsd.edu)

J. Willebrand, Institut für Meereskunde, Düsternbrooker Weg 20, 24105 Kiel, Germany. (jwillebrand@ifm.uni-kiel.de)